

# EFFICIENT NON-FOURIER IMPLEMENTATION OF LANDAU-FLUID OPERATORS IN THE BOUT++ CODE

A. M. Dimits, I. Joseph, M. V. Umansky, P. W. Xi,\* X. Q. Xu, LLNL

Presented at the 54th Annual Meeting of the APS Division of Plasma Physics  
Providence, RI, Oct 30, 2012



\*also, School of Physics, Peking University

Work performed for U.S. DOE by LLNL under Contract DE-AC52-07NA27344

# Motivation and Introduction

- Effective phase-mixing damping rate in Landau-fluid closure

$$\gamma \propto -|k_{\parallel}| v_{\text{th}}$$

- Specific example, with collisions

$$\nabla_{\parallel} Q_{\parallel}(z) \approx -8n_0 v_{\text{th}}^2 \int dk_{\parallel} e^{ik_{\parallel} z} \frac{k_{\parallel}^2 \tilde{T}_{\parallel}}{\sqrt{8\pi} |k_{\parallel}| v_{\text{th}} + (3\pi - 8) \nu_s}$$

- Such operators are easy to represent and efficient to calculate in Fourier ( $k_{\parallel}$ ) space.
- When large (including background) spatial inhomogeneities are present in the phase-mixing operators, evaluation using Fourier methods becomes inefficient.

- With mesh-based schemes (finite difference, volume, element, etc.), it is straightforward to construct approximations to  $(\nabla_{||})^n \leftrightarrow (ik_{||})^n$ , but harder for, e.g.,  $|k_{||}| \times k_{||}^n = \text{sgn}(k_{||}) \times k_{||}^{n+1}$ .
  - ▶ not local in configuration space
- Direct use of the corresponding discretized configuration space kernel by convolution or matrix multiplication is potentially expensive.
  - ▶  $N_g^2$  scaling vs.  $N_g \log(N_g)$  of computational expense
- **ACCURATE APPROXIMATIONS ARE POSSIBLE THAT CAN BE IMPLEMENTED WITH FOURIER-LIKE SCALING.**

# Basic idea

- Approximate  $1/|k|$  as a sum of suitably scaled Lorentzians

$$\frac{1}{|k|} \approx \sum_{n=0}^N \frac{\alpha^n}{k^2 + \alpha^{2n}}$$

- Each individual component of the sum has the correct parity, but asymptotic dependence  $1/k^2$  for large  $k$ .
- With the above scaling of the height and width, successive terms approximately “fill in” successively higher parts of the  $1/|k|$  curve
- The sum provides a quite good fit over some spectral range, which increases with  $N$
- Lorentzians in  $k$  space are inverses of Helmholtz operators in real space

# Approximate calculation

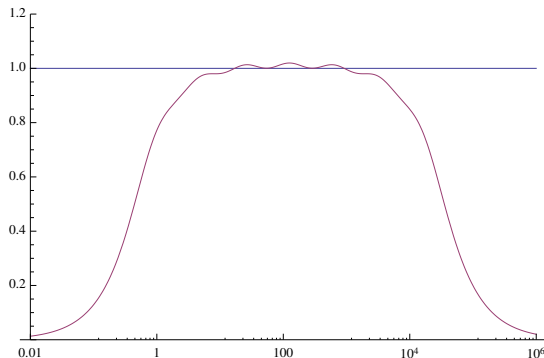
- Discretize the Helmholtz equations
- Solve via a tridiagonal (for 2-point differences) or banded (for higher-order differences) matrix solution
- Direct solvers should work well
  - ▶ the matrices are well conditioned
  - ▶ parallelizeable along direction of solve
- Sum the results of the matrix solves

# Accuracy of the basic approximation

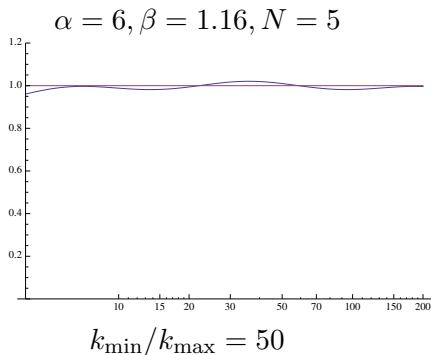
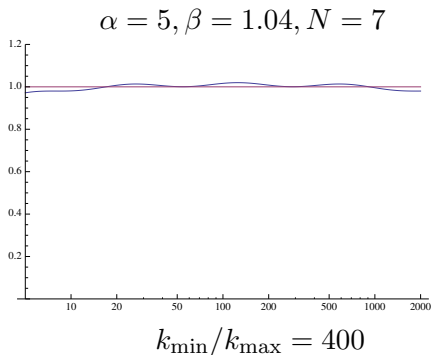
- Look at how close to  $\text{sgn}(k) = k/|k|$  is

$$\psi(k; \alpha, \beta, N) = \beta k \sum_{n=0}^{N-1} \frac{\alpha^n}{k^2 + \alpha^{2n}} ?$$

- $\alpha = 5, \beta = 1.04, N = 7$



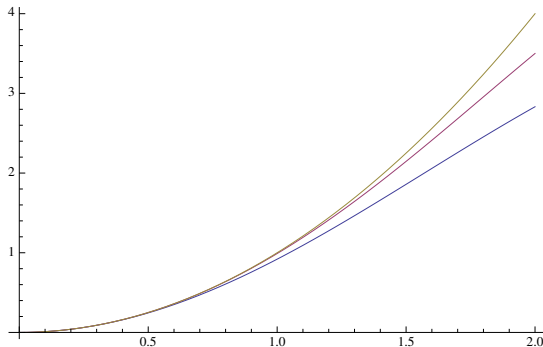
# Accuracy of the basic approximation



## Finite-grid effects

Compare exact, 3-point and 5-point approximations to  $k^2$

$$K_2^2(k\Delta) = [2 \sin(k\Delta/2)/\Delta]^2$$
$$K_4^2(k\Delta) = \frac{4}{3} [2 \sin(k\Delta/2)/\Delta]^2 - \frac{1}{3} [\sin(k\Delta)/\Delta]^2$$





# Finite-grid effects

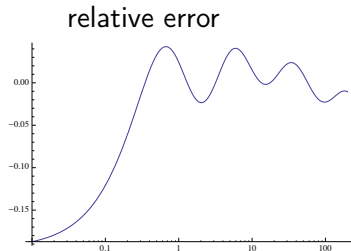
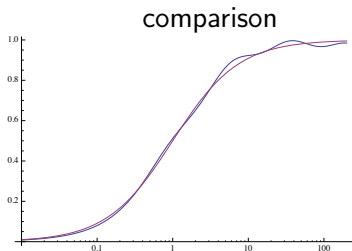
- Finite differences good to some  $k_d = \hat{k}_d/\Delta$  ;  $k_d \approx 0.8$  for 3-point;  $k_d \approx 1.6$  for 5-point
- Given  $\psi(\hat{k})$  which fits the desired operator well for  $\hat{k}_{min} \lesssim \hat{k} \lesssim \hat{k}_{max}$ , scale  $\hat{k}$  by factor  $\lambda$  so that  $\lambda\hat{k}_{max} = \hat{k}_d/\Delta$ , i.e.,  $\lambda = \hat{k}_d/(\hat{k}_{max}\Delta)$ .
- Then  $\psi(k/\lambda) = \psi(k\Delta\hat{k}_{max}/\hat{k}_d)$  gives a good fit for  $\hat{k}_d\hat{k}_{min}/\hat{k}_{max} \lesssim k\Delta \lesssim \hat{k}_d$ , i.e., for all modes in system for  $L \lesssim 2\Delta\hat{k}_{max}/\hat{k}_{min}$ .

# Include collisions

- Can scale operator fit problem to obtaining a fit to  $k/(|k| + 1)$
- Can obtain reasonable fit by adjusting coefficient of first Lorentzian

$$\psi(k; \alpha, \beta, N) = \beta k \left[ \frac{\eta}{k^2 + 1} + \sum_{n=1}^N \frac{\alpha^n}{k^2 + \alpha^{2n}} \right]$$

- $\alpha = 6, \beta = 1.15, N = 5, \eta = 0.5$



# Implementation

- Non-Fourier approximation to  $1/|k|$  and  $-|k|$  operator.

$$\begin{aligned} 1/|k| &\approx \beta \sum_{n=0}^N \frac{\alpha^n}{k^2 + (\alpha^n k_0)^2} \\ -|k| &= -\frac{k^2}{|k|} \approx -\beta \sum_{n=0}^N \alpha^n + \beta \sum_{n=0}^N \frac{\alpha^{3n} k_0^2}{k^2 + (\alpha^n k_0)^2} \end{aligned}$$

- Use 3-point second difference for second derivative

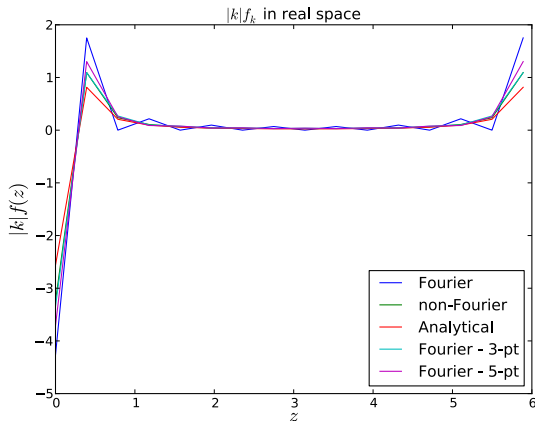
$$\begin{aligned} \frac{\partial^2 \psi}{\partial z^2} &\rightarrow \frac{1}{\Delta^2} (\psi_{i+1} + \psi_{i-1} - 2\psi_i) \\ \therefore k^2 &\rightarrow K_2^2(k\Delta) = [2 \sin(k\Delta/2)/\Delta]^2 \end{aligned}$$

- Periodic domain; "periodic tridiagonal" routine.

# Spatial Oscillations (Gibbs Phenomenon) for $-|k|$ Operator

- $\alpha = 5, N = 7, \beta = 1.04$ .
- System length =  $2\pi$  ; 16 grid cells

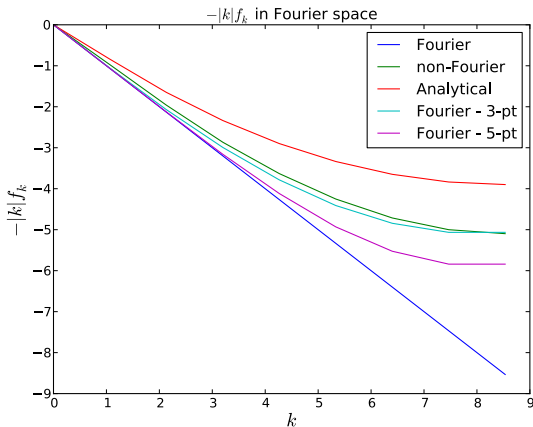
Real Space



# Spatial Oscillations (Gibbs Phenomenon) for $-|k|$ Operator

- $\alpha = 5, N = 7, \beta = 1.04$ .
- System length =  $2\pi$  ; 16 grid cells

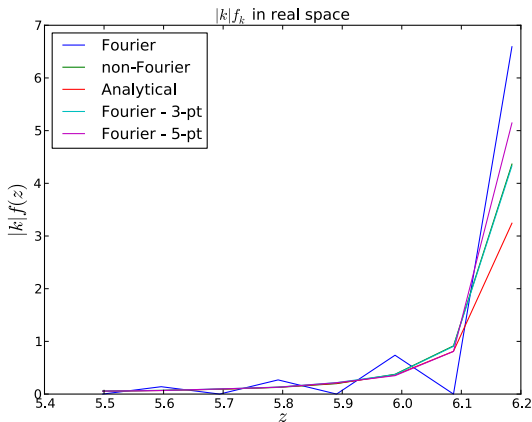
## Fourier Space



# Spatial Oscillations (Gibbs Phenomenon) for $-|k|$ Operator

- $\alpha = 5, N = 7, \beta = 1.04$ .
- System length =  $2\pi$  ; 16 grid cells

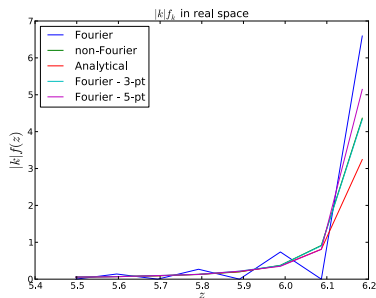
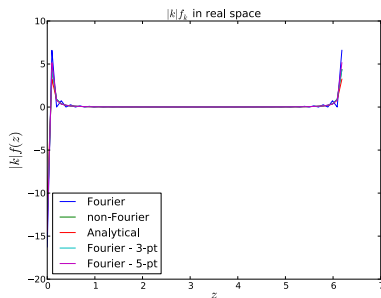
Real Space



# Spatial Oscillations (Gibbs Phenomenon) for $-|k|$ Operator

- $\alpha = 5, N = 7, \beta = 1.04$ .
- System length =  $2\pi$  ; 64 grid cells

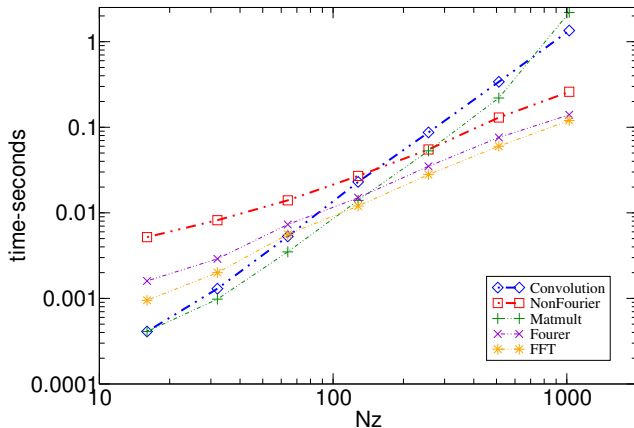
## Real Space



# Non-Fourier has similar computational scaling to Fourier

- Non-Fourier, with fixed  $N$ , scales as  $N_z$ , c.f.  $N_z^2$  for direct convolution
- Crossover point is at  $N_z \approx 128 \Rightarrow$  advantage for  $N_z \gtrsim 200$ .

Timings





# Collocation solution for Laplace inversion ansatz: $\eta_j(k) = b^j / (k^2 + b^{2j})$

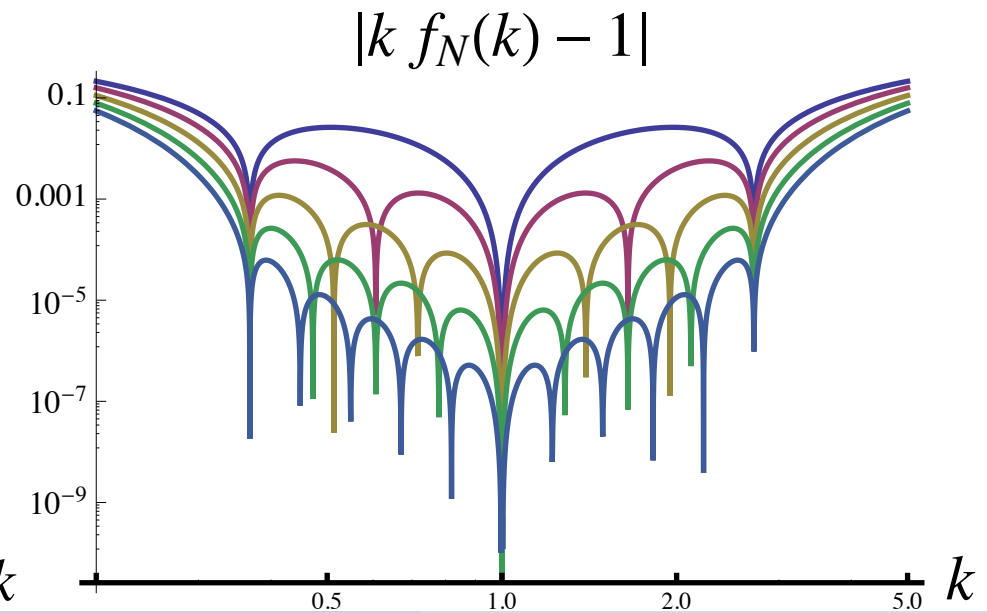
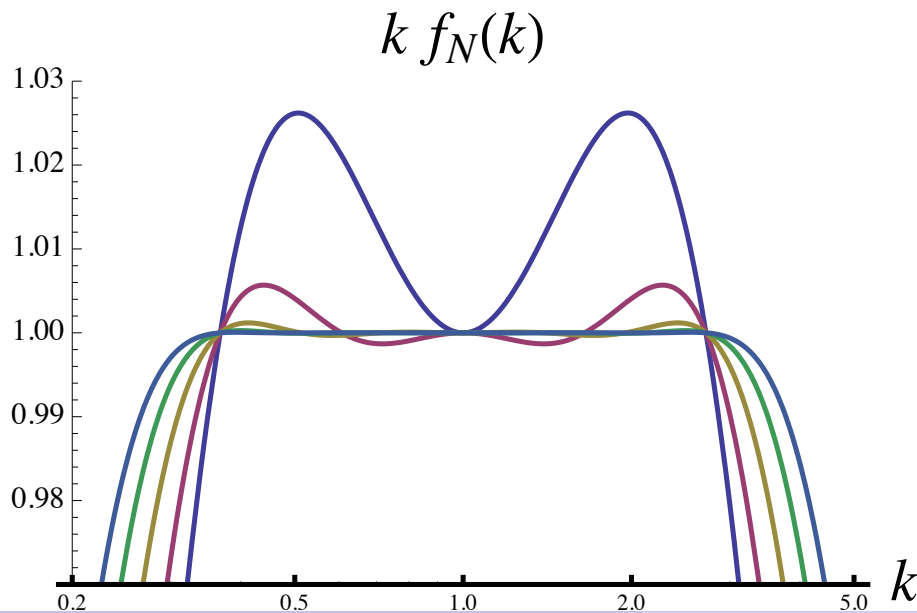
- Collocation at uniformly spaced points  $b^i$ , for  $i = -N, \dots, N$  lead to the symmetric linear problem  $Ma = 1$  where

$$M_r^s = b^r b^s / (b^{2r} + b^{2s})$$

- For  $b = e$  the solutions are

$N$	$2N + 1$	$[a^r]$
1	3	[1.84807, 1.68115, 1.84807]
2	5	[1.54322, 0.866876, 1.04278, 0.866876, 1.54322]
3	7	[1.53232, 0.300129, 0.811828, 0.575391, 0.811828, 0.300129, 1.53232]
4	9	[1.70273, -0.263771, 0.885701, 0.293448, 0.656293, ...]
5	11	[2.01764, -0.999102, 1.27026, -0.110205, 0.727017, 0.127763, ...]

- However, error grows at edges of logarithmic interval



# Uniform accuracy can be obtained with Chebyshev collocation points

- Chebyshev polynomial approximation can generate uniform error convergence over the logarithmic interval**

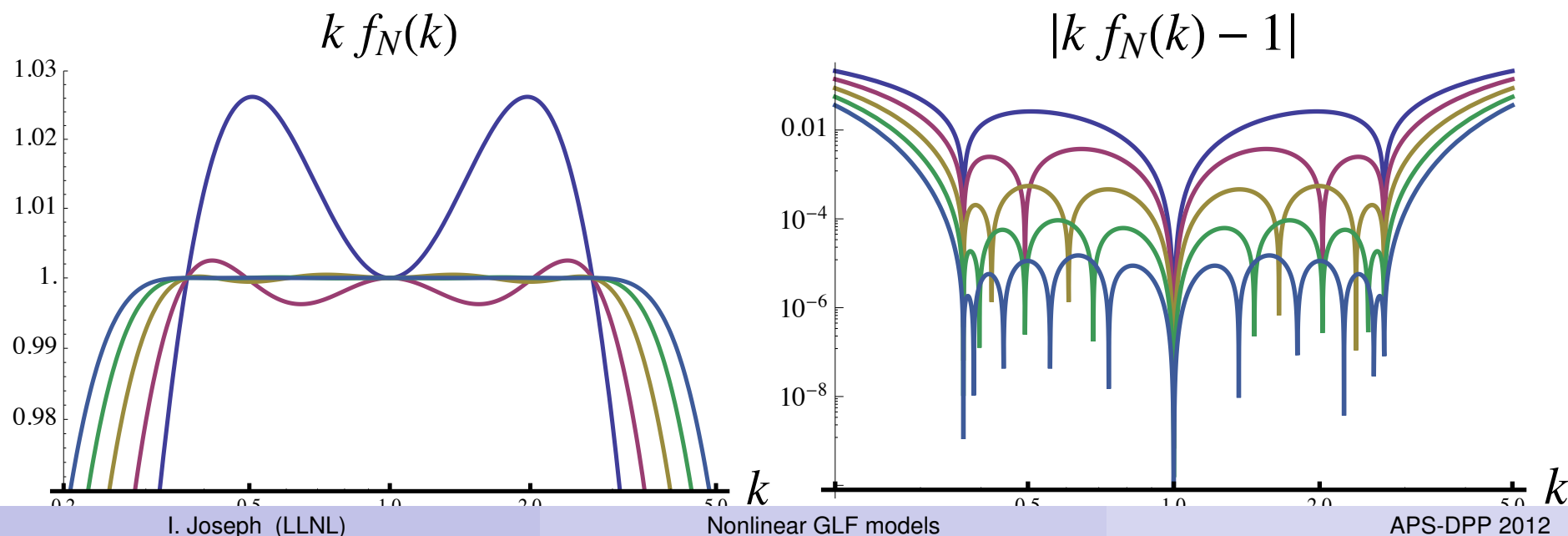
- For exponential interval  $b^N$ , first renormalize by taking the logarithm  $\beta = \beta_0 \log b$
- The Chebyshev collocation points  $\beta_s$  with  $2N + 1$  polynomials,  $s = -N, \dots, N$ , are

$$\beta_s = \cos((s - N)\pi/2N) \quad \rightarrow \quad b_s = \exp(\beta_0 \cos((s - N)\pi/2N))$$

- Chebyshev solution for  $\beta_0 = 1$ :**

$N$	$2N + 1$	$[a^j]$
1	3	[1.6529, -0.142332, 1.6529]
2	5	[4.06838, -3.65237, 2.52162, -3.65237, 4.06838]
3	7	[16.8245, -22.0064, 9.92733, -5.95441, 9.92733, -22.0064, 16.8245]
4	9	[82.5576, -124.155, 62.226, -30.1305, 22.6809, ...]
5	11	[445.908, -720.514, 409.297, -199.35, 110., -86.8868, ...]

- Maximum error is similar, but now more uniform over logarithmic interval**



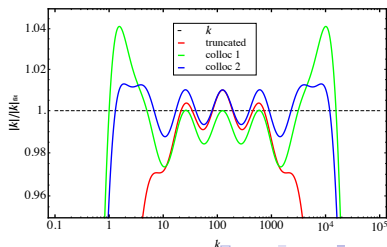
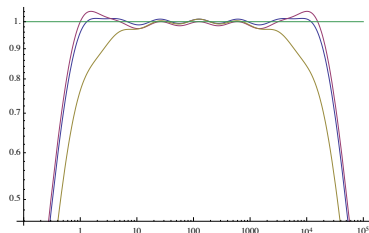
# Systematic collocation analysis → improved fits: collisionless

- Collisionless - good (near best) fit is of the form

$$1/|k| \approx \beta \sum_{n=1}^N \frac{\zeta_n}{k^2 + (\alpha^{n-1} \kappa_0)^2},$$

- Match exact and approximate forms at collocation points  $k = k_n$ ,  $k_n = \alpha^{n-1} \kappa_0$ ,  $n = 2, 3, \dots, N-1$ ,  $k_0 = \kappa_0/\eta$ ,  $k_N = \eta \alpha^{N-1} \kappa_0$ .
- matrix problem that can be handled e.g., by Mathematica
- Extends spectral range of good fit by  $\sim 10$ - $100$  for given  $N, \alpha$ .

Improved fits vs. original fit



# Collisional case introduces a scale length, the mean-free path: $\lambda$

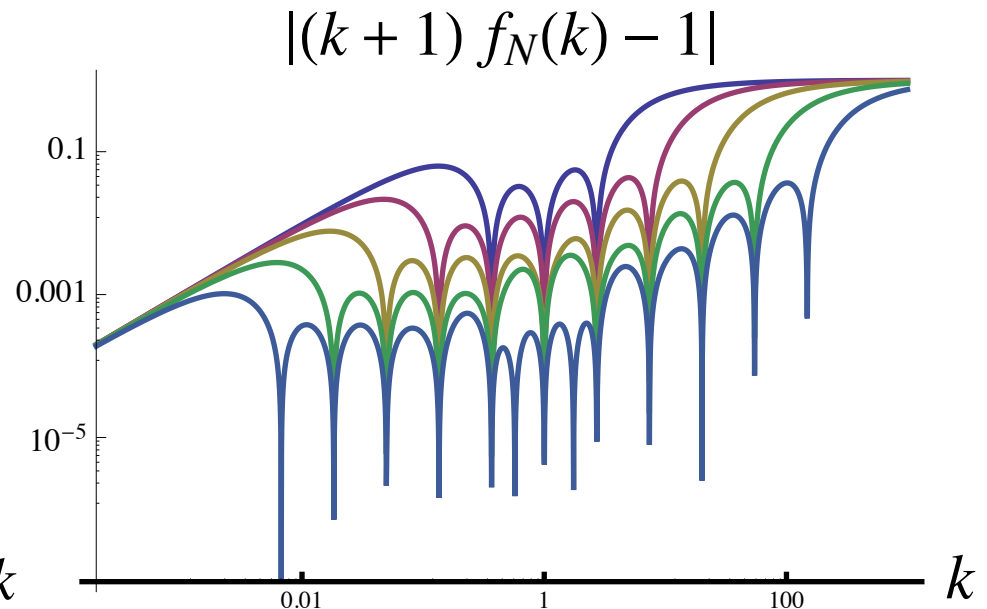
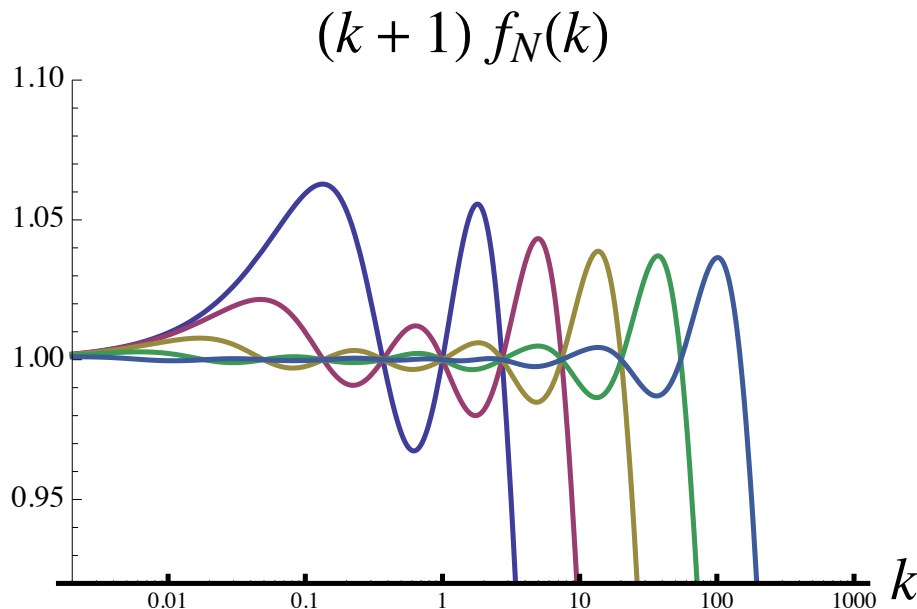
- **Key dimensionless parameter:**  $b = k_{max} \lambda$
- **Now, collocation at points  $k\lambda = b^s$  for  $s = -N, \dots, N$  generates the equation**

$$M_r^s a^r = b^s / (i + b^s)$$

- **For  $b = e$  the solutions are**

$N$	$2N + 1$	$[a^j]$
1	3	[0.19703, -0.0711661, 1.45587]
2	5	[0.0280711, 0.0210288, 0.470837, 0.155383, 1.53263]
3	7	[0.00382669, 0.00401212, 0.0966353, 0.261622, 0.714043, 0.219054, 1.5438]

- **Again, error grows for the limit  $k\lambda \gg 1$**



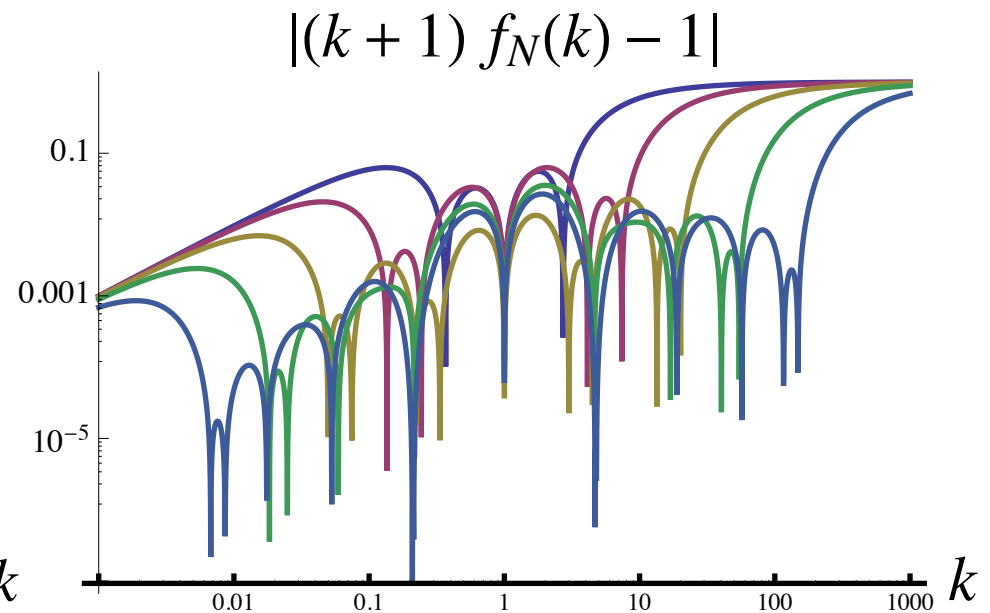
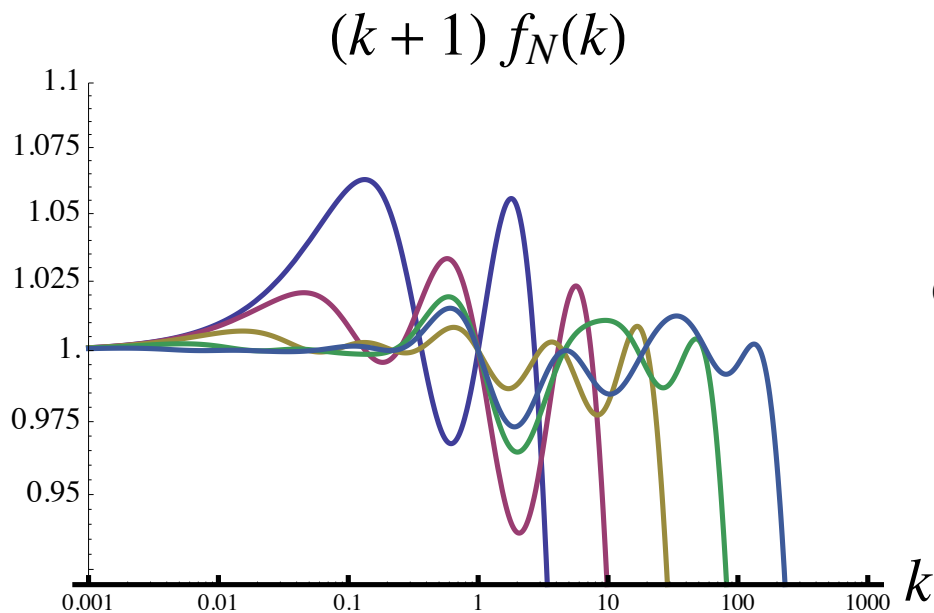
# Chebyshev collocation reduces error at large $k \sim k_{max}$

- **Perform collocation at points**  $k\lambda = \exp(s\beta_s)$   
**where**  $\beta_s = \cos((s - N)\pi/2N)$  **and**  $s = -N, \dots, N$

- **For  $b = e$  the solutions are**

$N$	$2N + 1$	$[a^j]$
1	3	[0.19703, -0.0711661, 1.45587]
2	5	[0.0308817, -0.00571965, 0.590679, -0.0967698, 1.68609]
3	7	[0.00571954, -0.00531807, 0.0514562, 0.451945, 1.03353, -0.960316, 2.30743]

- **Still may want to reduce error in middle of domain further ...**



# Systematic collocation analysis $\rightarrow$ improved fits: collisional

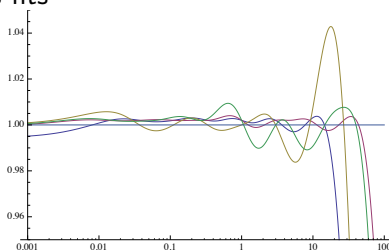
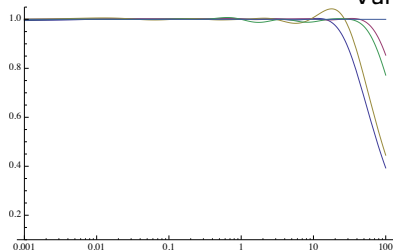
- Good (near best) fit is of the form

$$1/(1+|k|) \approx \beta \sum_{n=-N}^N \frac{\zeta_n}{k^2 + \alpha^{2n}},$$

► collocation points:  $k_n = \alpha^n$ ,  $n = -N, \dots, N-1$ ,  $k_N = \eta\alpha^N$ .

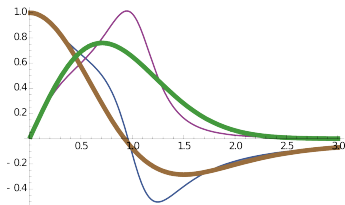
- $\alpha = 3, 4$ ;  $N = 3, 4$ ;  $\eta = 0.5, 0.6, 1$ .

Varous fits



# Effect of using sum of Lorentzians on the response functions

- We have implemented a set of Mathematica scripts, which reproduce the HP90 analytic calculations, and also modified them to give the effect of using the sum of Lorentzians for  $k/|k|$ .



Using exact  $k/|k|$  reproduces the HP90 3-field model.

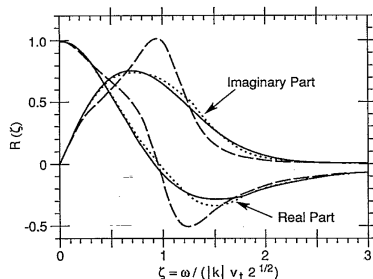
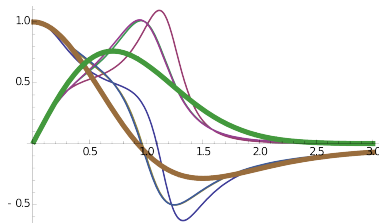


FIG. 1. The real and imaginary parts of the normalized response function  $R(\zeta) = -\bar{n}T_0/n_0e\bar{\phi}$  vs the normalized frequency  $\zeta$ . The solid lines are the exact kinetic result for a Maxwellian,  $R(\zeta) = 1 + \zeta Z(\zeta)$ . The dashed lines are from the three-moment fluid model with  $\Gamma=3$ ,  $\mu_1=0$ , and  $\chi_1=2/\sqrt{\pi}$ . The dotted lines are from the four-moment model.

# Replacing $k/|k|$ by the sum of Lorentzians approximation yields good fits to the Landau-fluid response functions

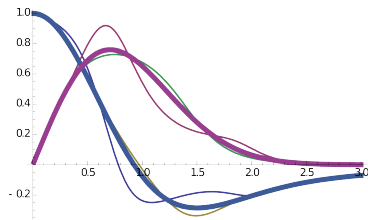
Effect of replacing  $k/|k|$  by sum of Lorentzians

3-fluid



$R = R_3(k/k_0)$ , for  $k_0 = 1, 10, 100$ .

4-fluid



$R = R_4(k/k_0)$  for  $k_0 = 1, 100$ .

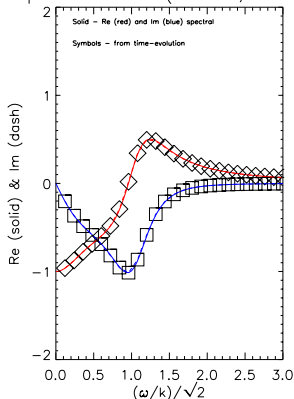


## Replacing $k/|k|$ by the sum of Lorentzians approximation yields good fits to the Landau-fluid response functions

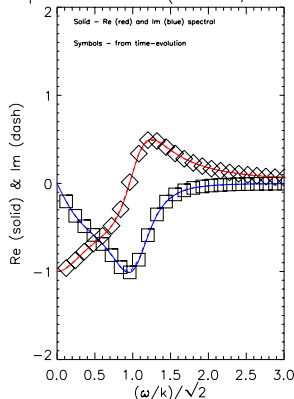
- considered local ( $q = -\chi \nabla T$ ) and nonlocal ( $q_k = -ik/|k| T k$ ) models for the spectral response function.
- The calculation is done by Fourier and non-Fourier methods, for comparison.
- Local non-Fourier means finite-difference, and nonlocal non-Fourier means the Lorentzian method (our main interest).
- Naming convention is: local/nonlocal  $\Leftrightarrow$  local=1/0, and similar for Fourier and non-Fourier.

Finite-difference and Fourier implementations of local (diffusive) heat flux in time evolution give response function in agreement with theoretical spectral analysis

Response function (local=0, fourier=0)

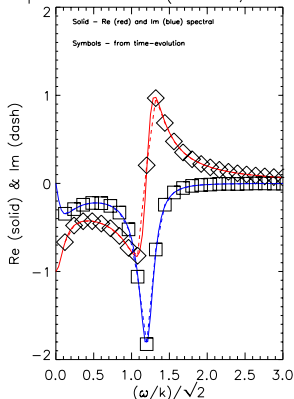


Response function (local=0, fourier=1)

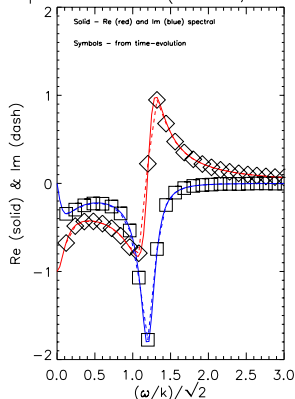


# Finite-difference and Fourier implementations of nonlocal heat flux in time evolution give response function in agreement with theoretical spectral analysis

Response function (local=1, fourier=0)

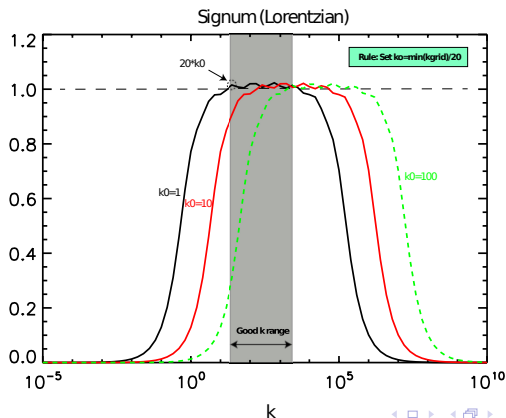


Response function (local=1, fourier=1)



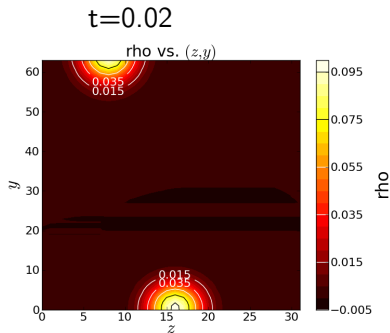
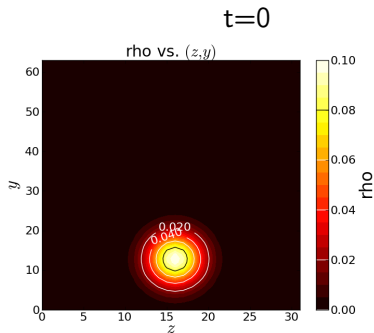
Normalizing wavenumber  $k_{z0}$  must be chosen to have region of good fit overlap with resolved modes

- $k_0 = K_0 * \text{zperiod}$ , where  $K_0$  is an  $O(1)$  multiplier
- e.g., for parallel case,  $\nabla_{||} = (1/h_y) \partial_y$ , so  $k_{||0} = K_{y0} / \sqrt{g_{yy}(y_0)}$ .  
 ▶  $\sqrt{g_{yy}(y_0)} = h_y(y_0)$  is a measure of the parallel connection length



# BOUT++ tests: Parallel advection across parallel boundary

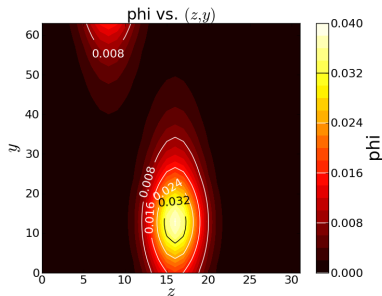
- Gaussian source pulse initialized away from parallel boundary advects across boundary with correct shift



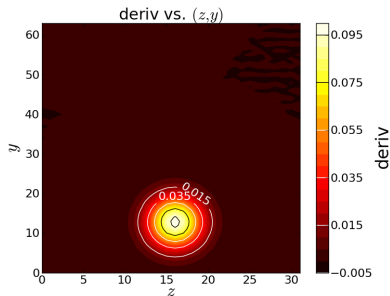
# BOUT++ tests: Parallel Laplace Solver

- Parallel (direction) Laplace solver gives sensible solutions with twist-shift boundary condition
- Reconstructed source function is consistent with original source function

Single Helmholtz inversion

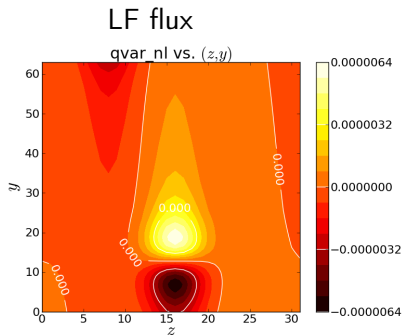
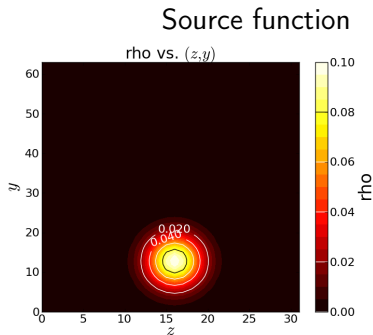


reconstructed source



# BOUT++ tests: Implementation of non-Fourier sum-of-Lorentzians for parallel Landau-fluid operator

- Non-Fourier LF operator gives sensible solutions with twist-shift boundary condition



## Toroidal Landau-fluid ( $|\omega_d|$ ) closure

- Example from Beer '96 - 3+1 equations:

$$\frac{du_{||}}{dt} = \text{stuff} - 4i\omega_d u_{||} - 2|\omega_d| \nu_5 u_{||}$$

$$\frac{dp_{||}}{dt} = \text{stuff} - i\omega_d (7p_{||} + p_{\perp} - 4n) - 2|\omega_d| (\nu_1 T_{||} + \nu_2 T_{\perp})$$

$$\frac{dp_{\perp}}{dt} = \text{stuff} - i\omega_d (5p_{\perp} + p_{||} - 3n) - 2|\omega_d| (\nu_3 T_{||} + \nu_4 T_{\perp})$$



# Toroidal Landau-fluid ( $|\omega_d|$ ) closure

- Linear forms for  $i\omega_d$

$$\begin{aligned} i\omega_d \Phi &= i\mathbf{V}_d \cdot \mathbf{k}_\perp \Phi \\ &= \frac{1}{2(T_{\text{norm}} B_0)} \left[ \frac{T_{\perp 0}}{B_0} \hat{\mathbf{b}} \times \nabla B_0 \cdot \nabla + T_{\parallel 0} \hat{\mathbf{b}} \times (\hat{\mathbf{b}} \cdot \nabla \hat{\mathbf{b}}) \cdot \nabla \right] \Phi \end{aligned}$$

- Need to add correct combination and generalize  $T_0$  to finite amplitude
- To get coefficients for modified version of *invert\_laplace*, decompose  $\mathbf{V}_d$  and  $\nabla \Phi$  into components

$$\begin{aligned} \mathbf{V}_d &= V_d^i \mathbf{e}_i \\ \nabla \Phi &= \mathbf{e}^i \partial_i \Phi \\ \mathbf{V}_d \cdot \nabla \Phi &= V_d^i \partial_i \Phi \end{aligned}$$

# BOUT++ implementation

- Components  $V_d^1$ ,  $V_d^3$  easily calculated with existing routines in BOUT++
- Basic Helmholtz equation can be solved using a modified version of existing perpendicular Laplace solver
  - ▶ Current equation is of the form

$$(c_1 k_z^2 - c_2 \partial_\psi^2 + c_3) \Phi = S$$

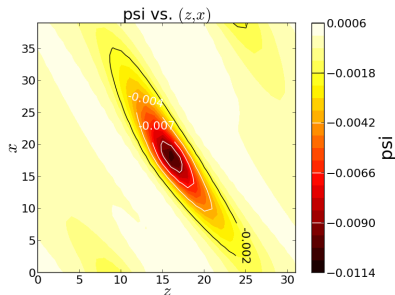
- ▶ Modify to solve

$$\left\{ \left[ (V_d^z)^2 k_z^2 - (V_d^\psi)^2 \partial_\psi^2 - 2i V_d^\psi V_d^z k_z \partial_\psi \right] + \alpha^2 (V_d^z)^2 k_{z0}^2 \right\} \Phi = S$$

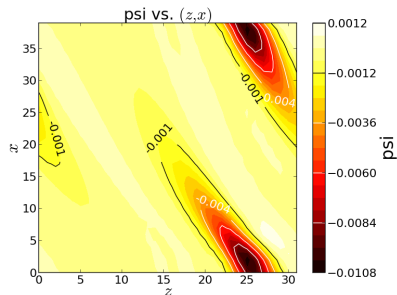
# BOUT++ tests: Perpendicular Laplace solver for $|\omega_d|$ terms

- Perpendicular (direction) Laplace solver gives sensible solutions
- Spreading by Helmholtz inversion is in the same direction as advection

Perp Helmholtz inversion t=0



Perp Helmholtz inversion t=8



(solutions with periodic radial BC's)

# Conclusions

- We have developed a new non-Fourier method for the calculation of Landau-fluid operators.
- Useful for situations with large (including background) spatial inhomogeneities.
- Good accuracy (relative error  $\lesssim 1\%$  over wide spectral range) is readily achievable.
- Computational cost has value and scaling similar to Fourier method.
- Considerable advantage over direct convolution or matrix multiplication for  $N_g \gtrsim 200$ .
- Readily applied to toroidal phase-mixing operators ( $|\omega_d|$ ).
- Method is also useful for capturing correct asymptotic form of gyrofluid operators.